Sequential assignments and secondary structure of the RNA-binding transcriptional regulator NusB

Amanda S. Altieri[1,a], Marie J. Mazzulla[a], Hongjun Zhou[a], Nina Costantino[b], Donald L. Court[b], R. Andrew Byrd[a]

[a] *Macromolecular NMR Section, P.O. Box B, Bldg. 538, ABL-Basic Research Program, NCI-Frederick Cancer Research and Development Center, Frederick, MD 21702, USA*

[b] *Molecular Control and Genetics Section, P.O. Box B, Bldg. 538, ABL-Basic Research Program, NCI-Frederick Cancer Research and Development Center, Frederick, MD 21702, USA*

Received 30 June 1997; revised version received 18 August 1997

Abstract The NusB protein is involved in transcriptional regulation in bacteriophage λ. NusB binds to the RNA form of the *nut* site and along with N, NusA, NusE and NusG, stabilizes the RNA polymerase transcription complex and allows stable, persistent antitermination. NusB contains a 10 residue Arg-rich RNA-binding motif (ARM) at the N-terminus but is not sequentially homologous to any other proteins. In contrast to other known ARM-containing proteins, NusB forms a stable structure in solution in the absence of RNA. NMR spectroscopy was used to determine that NusB contains six α-helices: R10–Q21, I27–F34, V45–L65, Q79–S93, Y100–F114 and D118–L127. The structure of NusB makes it a member of a newly emerging class of α-helical RNA-binding proteins.

Key words: Antitermination; Nus factor; NusB; RNA-binding protein; Secondary structure; Nuclear magnetic resonance

1. Introduction

One of the mechanisms of transcriptional regulation in bacteriophage λ is transcriptional antitermination, a process in which genes whose expression would be prematurely terminated are activated by termination suppression. In phage λ, genome-specific protein antiterminators convert RNA polymerase (RNAP) into a termination-resistant form during the early stages of elongation [1–3]. The N protein and host factors NusA, NusB, NusE and NusG associate with RNAP and the RNA form of the *nut* site (*nut* = BoxA+BoxB) to form a stable ribonucleoprotein (RNP) complex. This complex travels along the DNA distal to the *nut* site and allows transcription past potential termination sites [2]. A basal level of antitermination occurs with only the N and NusA proteins associated with the RNAP/nucleic acid complex [3,4]. However, stable, persistent antitermination requires the presence of the NusB, NusE and NusG factors as well [5].

NusB is a 16 kDa protein that binds selectively to BoxA of the nascent mRNA transcript as a heterodimer with the NusE protein [6,7]. A recent genetic study suggested that NusB interacts with BoxA RNA and that NusE is indirectly associated with the RNA [8]. This interaction of NusB with BoxA RNA is important, since a deletion of or mutations within BoxA that prevents the association of NusB/NusE with BoxA RNA also impairs antitermination [7]. The significance of NusB is also demonstrated by double-mutation studies in which a NusB mutant (*nusB101*) that can overcome suppression of antitermination caused by a NusA mutant (*nusA1*) requires BoxA RNA for this suppression [9]. One of the functions of NusB is to provide stabilization to the RNP antitermination complex and allow transcription farther downstream than in the absence of the Nus cofactors. It has also been shown that NusB counteracts an inhibitory factor in the cell that binds to the *nut* region [8]. The function of NusB would then be to compete with this cellular inhibitor for binding to BoxA and allow normal function of the antitermination complex. NusB has also been found to form a complex with ribosomal BoxA RNA and NusE, and may be involved in ribosomal RNA synthesis [2,7].

Structural details of RNA-binding proteins have lagged behind those of DNA-binding proteins. Several RNA-binding motifs have been identified in proteins with widely varied topology (reviewed in [10–12]). Many RNA-binding proteins carry multiple copies of a motif or contain several different motifs. Most sequence motifs for RNA-binding proteins have a mixed αβ structural topology. For example, the RNP motif has a βαββαβ topology [13–19] while the KH motif has a βααββα topology [20,21]. The double stranded RNA-binding (dsRNA) motif has an αβββα topology [22,23] and there are also RNA-binding motifs similar to the DNA-binding Zn-finger motif [24]. Another motif, the RGG box, is an Arg-Gly-Gly tripeptide repeated many times within the protein sequence [25,26] for which little is known about the structure. The Arg-rich RNA-binding motif (ARM) consists of small regions of the protein (10–20 amino acids) with a predominance of Arg residues. The sequence and structure of the ARM region in different proteins vary widely [27]. For example, the ARM region of BIV tat (ALGISYGRKKRRQRRRP) binds RNA as a β hairpin [28,29] whereas the ARM region of the Rev protein (TRQARRNRRRRWRERQ) binds RNA as an α-helix [30]. Many of the ARM proteins are unfolded in the absence of RNA and adopt a folded conformation upon binding [28,31,32]. A final example of topological variability is the recently identified S1 motif that forms a 5-stranded β-barrel [33].

The NusB protein contains an ARM motif but does not contain any other of the above mentioned motifs. NusB is not sequentially homologous to any known proteins based on a Basic Local Alignment Search Tool (BLAST) search

[1] Corresponding authors. Fax: (1) (301) 846-6231.
E-mail: http://www-brp.ncifcrf.gov/abl/msl/byrd.html

0014-5793/97/$17.00
PII S0014-5793(97)01128-9

[34]. In this paper, we show that in contrast to the other ARM proteins, NusB adopts a stable, folded structure in solution in the absence of RNA, with the exception of the ARM region itself (residues 1–10). We have determined the structure of NusB to be α-helical, which puts it into a class of RNA-binding proteins [35–37] that define a new, α-helical structural motif.

2. Materials and methods

2.1. Sample preparation

NusB was cloned into the pJL6 plasmid vector containing the pL promoter. The construct was transformed into NC198 cells that are N^+ and contain a temperature-sensitive repressor [1]. The transformed cells were grown in M9 minimal medium [38] supplemented with biotin, thiamine and 100 μg/ml carbenicillin. Preinduction growth was done at 32°C to an OD_{600} of 0.6–0.9 and cells were then induced at 42°C for 4 h. The harvested cells were homogenized in 8 M urea, 50 mM sodium phosphate and 20 mM dithiothreitol (DTT) at pH 6.8. The lysate was stirred for ~12 h at 4°C. The sample was centrifuged and the protein was isolated from the soluble fraction by FPLC using a 0–0.5 M NaCl gradient (with 8 M urea, 50 mM phosphate and 10 mM DTT at pH 6.8) on a HiLoad Sepharose SP cation exchange column. The NusB protein was then refolded by dialysis against decreasing amounts of urea in phosphate buffer. The protein was chromatographed on the same cation exchange column using the gradient described above without urea but with 5 mM DTT. The purified protein was then concentrated to final NMR sample concentrations of 1.0–1.5 mM in 50 mM sodium phosphate, 0.1 M NaCl and 2 mM DTT at pH 6.8. Isotopically labeled samples were prepared using the method described above except that $^{15}NH_4Cl$ (99.9% ^{15}N, Isotec), $^{13}C_6$-glucose (99% ^{13}C, Isotec), D_7-glucose (98% D, Cambridge Isotope Laboratories, Inc.) and D_2O (99.8% D, Isotec) were substituted as required.

The purity of the NusB preparation was verified using mass spectrometry, amino acid analysis and protein sequencing. The extent of isotopic label incorporation was 99.0% ^{15}N, 99.9% ^{13}C, ^{15}N and 99.94% ^2H, ^{15}N. The NusB protein produced by the above protocol is in its native conformation as shown by wild-type activity in an in vitro antitermination assay (A. Das, personal communication). The protein concentration was determined by amino acid analysis and UV absorbance at 280 nm. The extinction coefficient (ε_{280}) was determined to be 8.03 mM^{-1} cm^{-1}.

2.2. Circular dichroism (CD)

The CD spectrum was recorded on a Jasco 720 spectropolarimeter. The protein sample was 10.4 μM in 50 mM phosphate buffer with 2 mM DTT. Spectra were recorded from 180 to 260 nm using a 0.1 mm path length demountable cell (Uvonics) at 22°C. Ellipticity was calculated per residue.

2.3. NMR spectroscopy

All spectra were recorded on a 600 MHz Varian Unity Plus spectrometer equipped with triple-resonance pulsed field gradient (PFG) probes (Nalorac Corporation). An 8 mm diameter probe and sample was used for enhanced sensitivity in all of the sequential assignment experiments and in the 4D HMQC-NOESY-HSQC experiment. A 5 mm probe and sample was used in all of the other experiments.

^1H-^{15}N HSQC: Standard HSQC spectra were run using flipback pulses [39] and WATERGATE [40] for solvent suppression.

WATERSLED: Self-diffusion measurements of 1.2 mM NusB in 90% H_2O/10% D_2O were made using the WATERSLED sequence described in [41]. PFG calibration was carried out as described therein. The PFG strength was arrayed in 32 steps from 4 to 42 G/cm. The diffusion time was 134 ms and 128 transients were collected with a recycle delay of 10 s. Data were processed in Felix 2.30 (Biosym Technologies, Inc.). The MLAB program (Civilized Software, Inc.) was used to fit the integrated intensities (aliphatic region excluding peaks from excess DTT) to an exponential curve from which the self-diffusion coefficient D_s was obtained. The goodness of fit was determined by calculating the residual error of the experimental data to the fit curve.

CBCA(CO)NH, HNCACB, C(CO)NH and H(CCO)NH: The triple-resonance sequential assignment experiments were run using PFG-coherence selection pulse sequences with sensitivity enhancement [42]. Spectral details are shown in Table 1. Sequential assignments were made using Ansig 3.2 software [43,44] and were assisted by the assignment probability program of Grzesiek and Bax [45]. Side chain ^1H and ^{13}C assignments were made using the 3D triple resonance C(CO)NH and H(CCO)NH experiments [42] and a 3D HCCH-TOCSY experiment [46]. The sample for the HCCH-TOCSY experiment was 1.3 mM in 100% D_2O.

$^3J_{HNHA}$: The $^3J_{HNHA}$ coupling constants were measuring from a 3D HNHA experiment and the backbone dihedral angle, ϕ, was calculated using the modified Karplus equation [47]. The data were processed and analyzed using Felix 95 (Biosym Technologies, Inc.).

HN exchange: Amide exchange information was obtained by dissolving a lyophilized NusB sample into fresh 99.9% D_2O (Sigma) and observing the decrease in amide (NH) signals in a series of ^1H-^{15}N HSQC experiments over 24 h. The first spectrum was obtained 10 min after dissolving the sample in D_2O.

Nuclear Overhauser effect spectroscopy (NOESY): The following experiments were analyzed to obtain short-range NOEs indicative of secondary structure: a 3D ^{15}N-edited NOESY-HSQC [48], $\tau_{mix} = 125$ ms on 1.2 mM ^{15}N-NusB, a 4D (C/N) HMQC-NOESY-HSQC [49], $\tau_{mix} = 100$ ms on 1.5 mM ^{13}C,^{15}N-NusB, and a 4D (N/N) HSQC-NOESY-HSQC experiment [50,51], $\tau_{mix} = 200$ ms on a 1.7 mM ^2H,^{15}N-NusB sample. Flipback pulses and WATERGATE were used for solvent suppression in each of the NOESY experiments. Additional spectral parameters are shown in Table 1.

3. Results

3.1. Solution state characterization

The CD spectrum of NusB is shown in Fig. 1. A maximum at 191 nm and minima at 208 and 222 nm are consistent with α-helical secondary structure. The amplitude of the maximum is 65 000 deg cm^2 $dmol^{-1}$ and the amplitudes of both minima are −28 000 deg cm^2 $dmol^{-1}$. This spectrum corresponds to a folded protein with 80–85% α-helicity [52].

The NusB protein exists in solution as a monomer under NMR conditions. The monomeric state is confirmed by NMR PFG self-diffusion measurements, which are consistent with results from relaxation and line width measurements for a 16 kDa protein. The resulting self-diffusion coefficient, D_s, of 1.01×10^{-6} cm^2 s^{-1} corresponds to a monomer of NusB, by comparison to the D_s of two proteins of related size (lysozyme, 14.1 kDa, $D_s = 1.04 \times 10^{-6}$ cm^2 s^{-1}; monocyte chemotactic protein (MCP-1), 17.4 kDa dimer, $D_s = 1.08 \times 10^{-6}$ cm^2

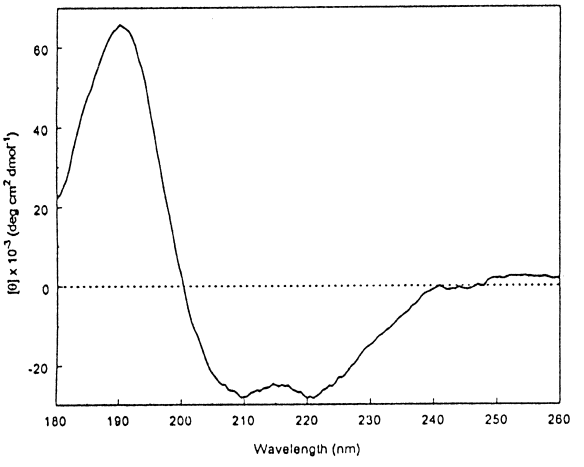

Fig. 1. The CD spectrum of 10.4 μM NusB in 50 mM phosphate buffer at pH 6.8 and 2 mM DTT. The data are consistent with 80–85% α-helicity [52].

Table 1
Acquisition parameters for the NMR experiments

Experiment	Sample	Nucleus				Complex time domain pts.				Spectral width (Hz)				Mix time (ms)	# scans	Expt. time (h)
		F1	F2	F3	F4	t1	t2	t3	t4	sw1	sw2	sw3	sw4			
CBCA(CO)NH [42]	1.3 mM $^{13}C,^{15}N$	$^{13}C_{a,b}$	^{15}N	$^{1}H_N$		50	32	1024		9259.3	1479.3	7504.7			32	63
HNCACB [42]	1.3 mM $^{13}C,^{15}N$	$^{13}C_{a,b}$	^{15}N	$^{1}H_N$		50	32	1024		9259.3	1479.3	7504.7			32	63
C(CO)NH [42]	1.3 mM $^{13}C,^{15}N$	^{13}C	^{15}N	$^{1}H_N$		50	32	1024		9259.3	1479.3	7504.7		22.8	32	63
H(CCO)NH [42]	1.3 mM $^{13}C,^{15}N$	$^{1}H_C$	^{15}N	$^{1}H_N$		54	32	1024		3876.0	1479.3	7504.7		23.5	32	68
HCCH-TOCSY [46]	1.3 mM $^{13}C,^{15}N$	$^{1}H_C$	^{13}C	$^{1}H_C$		128	48	1024		3600.0	3021.1	6504.1		22.8	8	60
HNHA [47]	1.0 mM ^{15}N	^{1}H	^{15}N	$^{1}H_N$		64	32	1024		4200.0	1479.3	7504.7			28	70
NOESY-HSQC [48]	1.0 mM ^{15}N	^{1}H	^{15}N	$^{1}H_N$		128	32	512		7518.8	2433.1	7523.0		125	4	41
HMQC-NOESY-HSQC [49]	1.3 mM $^{13}C,^{15}N$	$^{1}H_C$	^{13}C	^{15}N	$^{1}H_N$	62	16	14	256	3300.3	3021.1	1479.3	7504.7	100	4	136
HSQC-NOESY-HSQC [50,51]	1.7 mM $^{2}H,^{15}N$	$^{1}H_N$	^{15}N	^{15}N	$^{1}H_N$	32	16	16	256	2597.4	1479.3	1479.3	7504.7	200	4	164

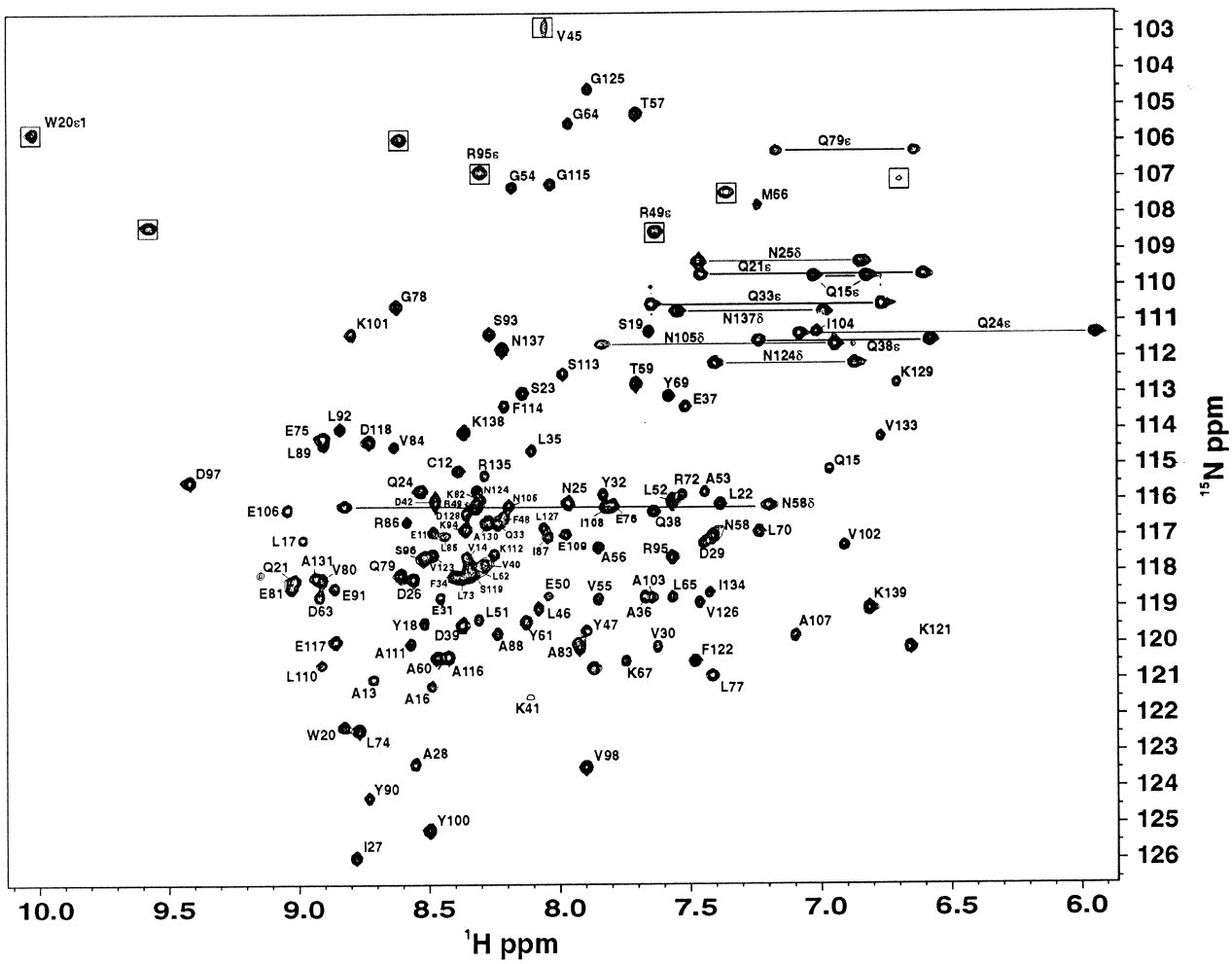

Fig. 2. ^{1}H-^{15}N HSQC spectrum of 1.7 mM $^{2}H,^{15}N$-NusB in 90% H_2O/10% D_2O at 600 MHz. Acquisition parameters: ^{1}H sweep = 7504.7 Hz, acquisition time = 136 ms, selective pulse for WATERGATE suppression scheme = 1.0 ms, flipback pulse = 2.5 ms, 4 scans per t1 increment, 128 t1 increments, ^{15}N sweep = 1479.3 Hz and States-TPPI [60] for quadrature in t1. Spectra were processed using NMRPipe [61]. Data were processed using time-domain solvent subtraction and were zero-filled and multiplied by a 90°-shifted squared sine-bell before Fourier transformation.

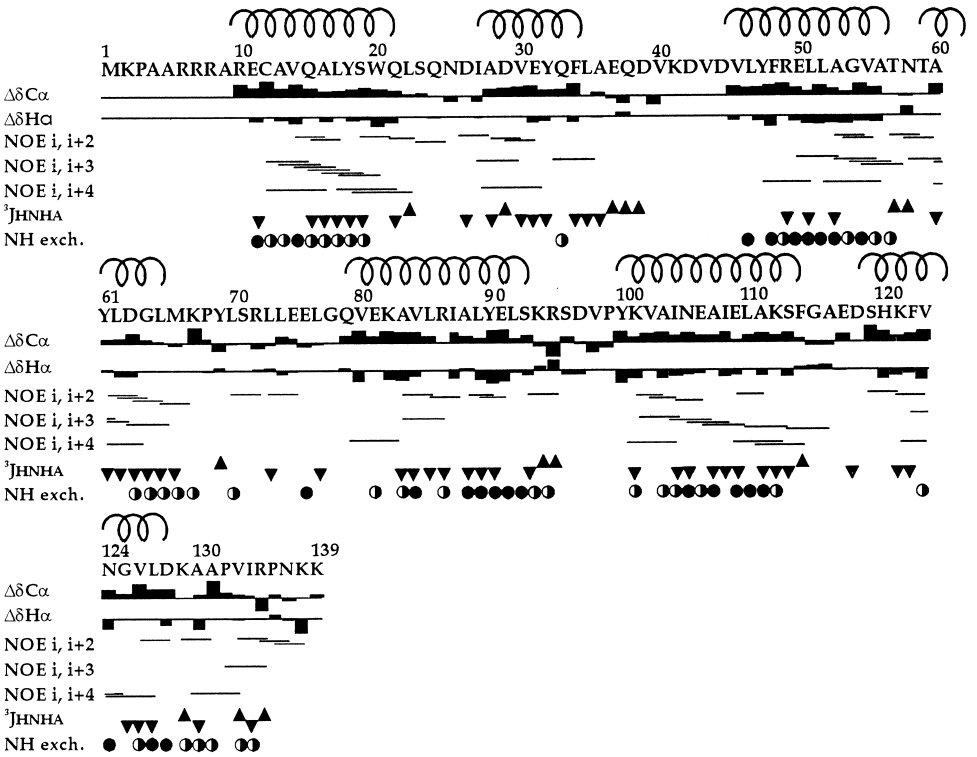

Fig. 3. Summary of secondary structure results for NusB. NOEs shown are a sum of NOEs found between backbone atoms (HN-HN, Hα-HN and Hβ-HN) of the indicated residues. Downward triangles are shown for residues with $^3J_{HNHA} < 6$ Hz and upward triangles for residues with $^3J_{HNHA} > 8$ Hz. Amide exchange results are also shown. Closed circles are for residues whose backbone HN is in slow exchange (still present after 24 h in D_2O solvent). Half-filled circles are shown for residues whose backbone HN is in intermediate-slow exchange (present after 2 h, but exchanged by 24 h). No symbol is indicated for residues whose HN had exchanged within 30 min. Helical symbols are shown above the sequence for regions that are determined to be α-helical based on the above data.

s^{-1}) and to a larger protein that would be approximately the size of a NusB dimer (interleukin-10, 37.4 kDa dimer, $D_s = 0.82 \times 10^{-6}$ cm^2 s^{-1}) [41]. Furthermore, the excellent fit of the experimental data to a single exponential curve supports the conclusion of a single, monomeric species in solution.

3.2. Sequential assignments

The ^1H-^{15}N heteronuclear single quantum correlation spectrum (HSQC) of perdeuterated NusB is shown in Fig. 2. The spectrum shows good chemical shift dispersion for the backbone amides (NH) of a 139 residue (16 kDa) protein. This dispersion as well as redundancy in the five 3D spectra used for sequential assignments yield complete, unambiguous assignments for the majority of the protein. The backbone amide cross peaks are labeled with their sequential assignments in Fig. 2. The side chain amides (NH_2) of the 11 Asn and Gln residues in NusB are shown as connected peaks. The Arg side chain Nε-Hε have been assigned for R49 and R95. The unlabeled folded cross peaks (boxed = folded peak) in Fig. 2 are from four additional Arg side chain Nε-Hε. The amide resonances V43, D44, S71, and H120 as well as for the ARM region, residues M1–R10, are not observed. The absence of these peaks is probably due to exchange broadening on an intermediate (∼ms) time scale which can be caused by solvent exchange or conformational variability [53]. The remaining backbone and side chain resonance assignments for ^1H, ^{13}C and ^{15}N nuclei have been completed and will be presented subsequently.

3.3. Secondary structure

Identification of secondary structure from NMR data takes advantage of several observable characteristics. With the complete sequential assignments, chemical shift differences from random coil values, Δδ, are calculated for the protein. The chemical shifts of Cα, Cβ, C′ and Hα nuclei are particularly sensitive to secondary structure in predictable ways [54–56]. Fig. 3 shows the measured Δδ for the Cα and Hα nuclei of NusB. The Δδ for Cα are downfield from random coil values and those for Hα are upfield from random coil values, consistent with a primarily α-helical secondary structure.

Backbone dihedral angles were obtained for the well-resolved HN to Hα resonances of NusB and are shown as $^3J_{HNHA}$ in Fig. 3. Downward arrows are shown for 52 residues whose $^3J_{HNHA} < 6$ Hz, corresponding to residues in α-helices ($\phi \sim -60°$). Upward arrows are shown for 14 residues whose $^3J_{HNHA} > 8$ Hz, corresponding to residues in a more extended or β conformation ($\phi \sim 120°$). These results show that much more α-helical secondary structure, rather than β-strand, is present in NusB.

A clear indication of secondary structure is found by observing patterns of nuclear Overhauser enhancements (NOEs) that correspond to distances between backbone protons of non-sequential residues. Sequential series of (i,i+2), (i,i+3) and (i,i+4) NOEs are observed in α-helices [53], those found for NusB are summarized in Fig. 3. Several regions have dαN(i,i+3) NOEs and measurable dNN(i,i+2), dNN(i,i+3) and dαN(i,i+4) NOEs indicative of stable α-helices.

Slowly exchanging amide protons are often found in re-

gions of stable secondary structure, both α-helices and β-sheets. The NH protons that did not exchange to deuterons within 2 h of dissolving a freshly lyophilized sample into D_2O are indicated by half-filled circles in Fig. 3 while those that had not exchanged by 24 h are shown as closed circles.

By combining the chemical shift index, $^3J_{HNHA}$, identification of slowly exchanging amide protons and patterns of NOEs, we have identified six α-helices in NusB. The α-helices extend from R10–Q21 (helix A), I27–F34 (helix B), V45–L65 (helix C), Q79–S93 (helix D), Y100–F114 (helix E) and D118–L127 (helix F) and are shown schematically above the amino acid sequence in Fig. 3. The direction of δΔ for N59, the large $^3J_{HNHA}$ for T57 and N58 and the absence of (i,i+3) NOEs originating on A56 or T57 indicate a break in helical structure at T57–T59. This kink in helix C will be further characterized during structural refinement.

4. Discussion

The NusB RNA-binding antitermination protein is a folded protein containing six α-helices in solution. The α-helical structure of NusB determined by NMR is consistent with the CD spectrum as well as with secondary structure prediction methods based on the amino acid sequence [57]. These results show that NusB is different from some other ARM proteins such as N [32], Nun [58] and homeodomain/DNA [31] that are entirely unfolded when not bound to RNA and then fold upon binding to RNA. In NusB, only the ARM region (residues 1–10) seems to lack an ordered structure, while the rest of the protein forms a stable structure. The lack of observable resonances for residues 1–10 in the absence of RNA suggests that a conformational change or stabilization may take place in the ARM region of NusB when it binds to RNA. The significance of the NusB structure in the absence of RNA, in terms of understanding its binding to RNA, is not obvious. However, proteins or peptides containing ARM regions that are unfolded in the absence of RNA do exhibit specific binding to RNA. This observation makes it likely that binding also involves some of the remaining protein scaffold [59]. The inclusion of residues outside the ARM region as part of the binding surface could also explain differences in the binding specificity of the ARM region, whose amino acid sequences vary widely in different proteins.

Three-dimensional structure determination of NusB is in progress in our laboratory and should provide insight into the presentation of the ARM region to RNA. Studies of NusB in the presence of BoxA RNA are also under way and may provide insight into the specificity of the protein-RNA interaction as well as determine whether the ARM region alone is responsible for binding or whether other parts of the NusB protein are also involved.

Acknowledgements: We thank Asis Das for conducting activity assays on NusB, Terry Copeland for amino acid analysis, Lewis Pannell for mass spectral analysis, Gary Cristoph for use of his CD spectropolarimeter, Peter Domaille and Per Kraulis for assistance with Ansig, Frank Delaglio for assistance with NMRPipe, Paul Dowling for programming assistance and Guy Montelione for valuable discussions. Research sponsored by the National Cancer Institute, DHHS, under contract with ABL. The contents of this publication do not necessarily reflect the views or policies of the Department of Health and Human Services, nor does mention of trade names, commercial products, or organizations imply endorsement by the U.S. Government.

References

[1] Das, A., Pal, M., Garcia-Mena, J., Whalen, W., Wolska, K., Crossley, R., Rees, W.A., vonHippel, P.H., Costantino, N., Court, D.L., Mazzulla, M.J., Altieri, A.S., Byrd, R.A., Chattopadhyay, S., DeVito, J. and Ghosh, B. (1996) Methods Enzymol. 274, 374–402.
[2] Greenblatt, J. (1992) in: Transcriptional Regulation (McKnight, S.L. and Yamamoto, K.R., Eds.) pp. 203–226, Cold Spring Harbor Laboratory Press, Cold Spring Harbor, NY.
[3] DeVito, J. and Das, A. (1994) Proc. Natl. Acad. Sci. USA 91, 8660–8664.
[4] Rees, W.A., Weitzel, S.E., Yager, T.D., Das, A. and von Hippel, P.H. (1996) Proc. Natl. Acad. Sci. USA 93, 342–346.
[5] Mason, S.W. and Greenblatt, J. (1991) Genes Dev. 5, 1504–1512.
[6] Mason, S.W., Li, J. and Greenblatt, J. (1992) J. Mol. Biol. 223, 55–66.
[7] Nodwell, J.R. and Greenblatt, J. (1993) Cell 72, 261–268.
[8] Patterson, T.A., Zhang, Z., Baker, T., Johnson, L.L., Friedman, D.I. and Court, D.L. (1994) J. Mol. Biol. 236, 217–228.
[9] Court, D.L., Patterson, T.A., Baker, T., Costantino, N., Mao, X. and Friedman, D.I. (1995) J. Bacteriol. 177, 2589–2591.
[10] Burd, C.G. and Dreyfuss, G. (1994) Science 256, 615–621.
[11] Mattaj, I.W. (1993) Cell 73, 837–840.
[12] Nagai, K. (1996) Curr. Opin. Struct. Biol. 6, 53–61.
[13] Swanson, M.S., Nakagawa, T.Y., LeVan, K. and Dreyfuss, G. (1987) Mol. Cell Biol. 7, 1731–1739.
[14] Oubridge, C., Ito, N., Evans, P.R., Teo, C.H. and Nagai, K. (1994) Nature 372, 432–438.
[15] Nagai, K., Oubridge, C., Jessen, T.H., Li, J. and Evans, P.R. (1990) Nature 348, 515–520.
[16] Hoffman, D.W., Query, C.C., Golden, B.L., White, S.W. and Keene, J.D. (1991) Proc. Natl. Acad. Sci. USA 88, 2495–2499.
[17] Avis, J.M., Allain, F.H.T., Howe, P., Varani, G., Nagai, K. and Neuhaus, D. (1996) J. Mol. Biol. 257, 398–411.
[18] Scherly, D., Boelens, W., Van Venrooij, W.J., Dathan, N.A., Hamm, J. and Mattaj, I.W. (1989) EMBO J. 8, 4163–4170.
[19] Wittekind, M., Gorlach, M., Friedrichs, M., Dreyfuss, G. and Mueller, L. (1992) Biochemistry 31, 6254–6265.
[20] Dejgaard, K. and Leffers, H. (1996) Eur. J. Biochem. 241, 425–431.
[21] Musco, G., Stier, G., Joseph, C., Castiglione Morelli, M.A., Nilges, M., Gibson, T.J. and Pastore, A. (1996) Cell 85, 237–245.
[22] Kharrat, A., Macias, M.J., Gibson, T.J., Nilges, M. and Pastore, A. (1995) EMBO J. 14, 3572–3584.
[23] Bycroft, M., Grunert, S., Murzin, A.G., Proctor, M. and St. Johnston, D. (1995) EMBO J. 14, 3563–3571.
[24] Pieler, T. (1994) in: RNA-Protein Interactions (Nagai, K. and Mattaj, I.W., Eds.) pp. 178–191, IRL Press, Oxford.
[25] Kiledjian, M. and Dreyfuss, G. (1992) EMBO J. 11, 2655–2664.
[26] Delattre, O., Zucman, J., Plougastel, B., Desmaze, C., Melot, T., Peter, M., Kovar, H., Joubert, I., deJong, P., Rouleau, G., Aurias, A. and Thomas, G. (1992) Nature 359, 162–165.
[27] Lazinski, D., Grzadzielska, E. and Das, A. (1989) Cell 59, 207–218.
[28] Calnan, B.J., Biancalana, S., Hudson, D. and Frankel, A.D. (1991) Genes Dev. 5, 201–210.
[29] Puglisi, J.D., Tan, R., Calnan, B.J., Frankel, A.D. and Williamson, J.R. (1992) Science 257, 76–80.
[30] Tan, R., Chen, L., Buettner, J.A., Hudson, D. and Frankel, A.D. (1993) Cell 73, 1031–1040.
[31] Wolberger, C. (1996) Curr. Opin. Struct. Biol. 6, 62–68.
[32] Van Gilst, M.R., Rees, W.A., Das, A. and von Hippel, P.H. (1997) Biochemistry 36, 1514–1524.
[33] Bycroft, M., Hubbard, T.J.P., Proctor, M., Freund, S.M.V. and Murzin, A.G. (1997) Cell 88, 235–242.
[34] Altschul, S.F., Gish, W., Miller, W., Myers, E.W. and Lipman, D.J. (1990) J. Mol. Biol. 215, 403–410.
[35] Markus, M., Hinck, A.P., Huang, S., Draper, D.E. and Torchia, D.A. (1997) Nat. Struct. Biol. 4, 70–77.
[36] Xing, Y., GuhaThakurta, D. and Draper, D.E. (1997) Nat. Struct. Biol. 4, 24–27.
[37] Berglund, H., Rak, A., Serganov, A., Garber, M. and Hard, T. (1997) Nat. Struct. Biol. 4, 20–23.
[38] Sambrook, J., Fritsch, E.F., Maniatis, T. (1989) Molecular Clon-

ing: A Laboratory Manual, 2nd edn., Cold Spring Harbor Laboratory Press, Cold Spring Harbor, NY.
[39] Grzesiek, S. and Bax, A. (1993) J. Am. Chem. Soc. 115, 12593–12594.
[40] Piotto, M., Saudek, V. and Sklenar, V. (1992) J. Biomol. NMR 2, 661–665.
[41] Altieri, A.S., Hinton, D.P. and Byrd, R.A. (1995) J. Am. Chem. Soc. 117, 7566–7577.
[42] Muhandiram, D.R. and Kay, L.E. (1994) J. Magn. Reson. Ser. B 103, 203–216.
[43] Kraulis, P.J. (1989) J. Magn. Reson. 84, 627–633.
[44] Kraulis, P.J., Domaille, P.J., Campbell-Burke, S.L., vanAken, T. and Laue, E.D. (1994) Biochemistry 33, 3515–3531.
[45] Grzesiek, S. and Bax, A. (1993) J. Biomol. NMR 3, 185–204.
[46] Kay, L.E., Xu, G.-Y., Singer, A.U., Muhandiram, D.R. and Foreman-Kay, J.D. (1993) J. Magn. Reson. Ser. B 101, 333–337.
[47] Vuister, G.W. and Bax, A. (1993) J. Am. Chem. Soc. 115, 7772–7777.
[48] Kay, L.E., Keifer, P. and Saarinen, T. (1992) J. Am. Chem. Soc. 114, 10663–10665.
[49] Kay, L.E., Clore, G.M., Bax, A. and Gronenborn, A. (1990) Science 249, 411–414.
[50] Venters, R.A., Metzler, W.J., Spicer, L.D., Mueller, L. and Farmer II, B.T. (1995) J. Am. Chem. Soc. 117, 9592–9593.
[51] Grzesiek, S., Wingfield, P., Stahl, S., Kaufman, J.D. and Bax, A. (1995) J. Am. Chem. Soc. 117, 9594–9595.
[52] Greenfield, N. and Fasman, G.D. (1969) Biochemistry 8, 4108–4116.
[53] Wuthrich, K. (1986) in: NMR of Proteins and Nucleic Acids, John Wiley and Sons, New York, NY.
[54] Wishart, D.S. and Sykes, B.D. (1994) J. Biomol. NMR 4, 171–180.
[55] Spera, S. and Bax, A. (1991) J. Am. Chem. Soc. 113, 5490–5492.
[56] Wishart, D.S., Sykes, B.D. and Richards, F.M. (1992) Biochemistry 31, 1647–1651.
[57] Rost, B. (1996) Methods Enzymol. 266, 525–539; Rost, B. and Sander, S. (1993) J. Mol. Biol. 232, 584–599; Rost, B. and Sander, S. (1994) Proteins 19, 55–72. The secondary structure prediction program PHDsec calculated NusB to contain 81.3% α-helix.
[58] Chattopadhyay, S., Hung, S.C., Stuart, A.C., Palmer III, A.G., Garcia-Mena, J., Das, A. and Gottesman, M.E. (1995) Proc. Natl. Acad. Sci. USA 92, 12131–12135.
[59] Varani, G. (1997) Acc. Chem. Res. 30, 189–195.
[60] Marion, D., Ikura, M., Tschudin, R. and Bax, A. (1989) J. Magn. Reson. 85, 393–399.
[61] Delaglio, F., Grzesiek, S., Vuister, G.W., Zhu, G., Pfeifer, J. and Bax, A. (1995) J. Biomol. NMR 6, 277–293.